The Synergistic Effects of Glacier Degradation and Oasis Expansion Affect Future Water Security Risks in Southern Xinjiang, China

Mingxia Ni [1], Muhtar Polat [2], Tingyu Sun [1], Jianxin Xia [1*]

[1] College of Life and Environmental Science, Minzu University of China, Beijing, 100081, PR China

[2]College of Tourism, Xinjiang University, Urumqi, 830049, PR China

Corresponding author: Jianxin Xia (jxxia@vip.sina.com)

Key Points:

- Glacial meltwater increased the available water resources of Southern Xinjiang oases and the buffer effect against drought may be deteriorated.
- Meltwater decreases and over-use of water resources will aggravate future water security risks in next decades.

Abstract

Global warming has led to significant glacier retreat around the Tarim River Basin and an increase in glacier meltwater. This has resulted in a rise in water resources in southern Xinjiang. Meanwhile, the development of human society has driven a substantial increase in water consumption for both production and daily living. This has disrupted the regional water supply-demand balance, making the risk of water resource stress more prominent. Given the characteristics of water resources utilization in arid areas and taking into account the changing trends in precipitation, glacial meltwater, and runoff due to climate change, along with population and economic development in southern Xinjiang, we employed the water stress index method to assess the current situation and potential future changes in water stress in the three regions of southern Xinjiang. The results indicated the following: The combined effects of precipitation and glacial meltwater have significantly increased river runoff, resulting in increased available water. The total water demand in the Aksu and Kashgar regions has shown a substantial increase, while the Hotan region has experienced a decrease in total water demand. The Aksu and Kashgar regions have exhibited an upword trend in water stress, while the Hotan region has seen some relief. Nevertheless, all the three regions in southern Xinjiang still face high water stress levels. In comparison to the historical period (2000-2020), the available water and total water demand in the three regions of southern Xinjiang are projected to increase during the next four periods (2030s, 2050s, 2070s and 2090s) under the SSP2-4.5 and SSP5-8.5 scenarios of the CMIP6 model. However, the rate of increase varies, and water stress exhibits different trends. Notably, the Aksu region is expected to face increasing water stress, indicating a significant risk of water scarcity and insecurity in the future.

Plain Language Summary

In recent years, under the background of climate warming, the rapid changes in water resources in southern Xinjiang, coupled with the increasing water demand for human activities, have made the risk of water stress in the region increasingly prominent. In order to understand the status and future changes of water stress in southern Xinjiang, we used the water stress index method to evaluate the water stress status and possible future changes in three regions of southern Xinjiang. As the temperature rises in southern Xinjiang, the surrounding mountain glaciers are melting more and more. Glacier melt water, which is the main source of runoff, has increased, and the amount of available water resources in the region has also increased. In the short term, the increase in water resources is good news, but in the long term, glaciers continue to retreat, ice volumes gradually decline, and glacier meltwater will gradually decrease after reaching its peak. At the same time, oases expand, especially human activity areas. As the area of cultivated land increases, the demand for water resources also increases sharply. In the extreme drought years and continuous drought years, without the buffering and regulating role of glaciers, southern Xinjiang will face huge risks of water stress.

1 Introduction

Water security is under global threat due to climate change, which accelerates evapotranspiration and the melting of the cryosphere, leading to the instability of water resource availability. Simultaneously, rapid growth in social and economic water demand places significant pressure on water resources. The water security of oases in southern Xinjiang faces a dual challenge. In the alpine-oasis-desert system, water resources play a crucial role in sustaining oasis development (Cheng et al., 2009, Chen et al., 2011). Under the combined influence of

climate change and human activities, the future water security in southern Xinjiang is at great risk, potentially leading to water scarcity similar to the historical tragedy of Gu Loulan due to water shortages.

Climate change is a primary factor driving changes in regional water scarcity (Gosling et al., 2016, Liu et al., 2019). As global temperatures continue to rise, the cryosphere is diminishing (IPCC, 2019), resulting in increased meltwater runoff (Chen et al., 2014, Penna et al., 2014, Sun et al., 2019). Southern Xinjiang, a typical arid region and China's primary inland river basin, relies significantly on glacial meltwater from mountainous areas as a key component of regional runoff. Due to climate and topographical factors, mountain glaciers are exceptionally sensitive to climate change (BACH et al., 2018), particularly in the inner Tarim River flow area, which offers the highest number of glaciers among the secondary watersheds in China (Liu et al., 2015). Projections suggest that by the end of the 21st century, glacier area in the arid northwest will decrease by 34% to 74% (Ding et al., 2020). Research has shown a 9.3% decline in glacier area in the Tarim River Basin from 1970 to 2008 (Shen et al., 2013), and a 25.88% decrease in the Aksu River Basin from 1975 to 2016 (Zhang et al., 2019). Glacier melt contributes significantly to increase runoff, for example, approximately two- thirds of the increased runoff in the Aksu River since 1960 can be attributed to glacial meltwater (Zhao et al., 2015). It is expected that meltwater runoff in the Yarkant River Basin will increase by 2050, resulting in a total runoff increase of roughly 13% to 35% (Zhang et al., 2012). Alongside increased precipitation, runoff in the Tarim River headwater basin has also risen (Immerzeel et al., 2010, Deng et al., 2019). However, as temperatures continues to rise and glaciers recede, a future meltwater peak (inflection point) is expected, after which glacier runoff will decline (Huss and Hock, 2018, Rounce et al., 2020, Sorg et al., 2012, Piao et al., 2010).

Southern Xinjiang is a critical node of the Silk Road Economic Belt in China. In recent years, with socioeconomic development, oases have been expanding (Liu et al., 2018, Zhuang et al., 2020). The oasis area in Xinjiang increased by 21.39% from 1972 to 2015 (He et al., 2018), and the artificial oasis on the southern margin of the Tarim Basin expanded by 1.28 times from 2000 to 2013 (Ren et al., 2015). The cultivated land area in artificial oases also grew significantly (Chen et al., 2022). Between1975 and 2015, cultivated land area in Xinjiang increased by 1.65 times (Wang et al., 2022). From 2000 to 2015, cultivated land area in southern Xinjiang increased by 5,110.07 km2 (Han et al., 2020), nearly doubling the cultivated land in the Aksu River Basin from 1991 to 2016 (Duan et al., 2021). In 2016, the cultivated area in Celle Oasis increased by 15.3% compared to 1970 (Liu et al., 2018). Cultivated land area in the middle reaches of the Kriya River Basin increased by 6.51% between 1995 and 2015 (Zubaidai et al., 2018). The expansion of cultivated land has increased the water demand. Agricultural water consumption on the northern slope of the Tianshan Mountains rose by 38.7% compared to 2010 (Tang et al., 2022), and irrigation water demand in the Heihe River Basin increased by 6.3% from 2000 to 2010 (Zhou et al., 2017). In 2015, the total water demand in the Kriya River Basin increased by 9.5% compared to 1995 (Zubaidai, 2019). However, despite increased runoff contributing to the water supply, runoff in the lower Tarim River continues to decrease (Hui Tao, 2011). Irrational exploitation and utilization have exacerbated the disparity between water resource supply and demand.

The stress on water resources, reflecting the balance between supply and demand, can be assessed using a water resource stress index. This assessment aids in clarifying the supply-demand relationship of regional water resources, revealing the extent of regional water resource

scarcity, and providing a scientific foundation for water resource management, security and sustainable development in the basin. It is estimated that two-thirds of the global population (4.0 billion people) live under conditions of severe water scarcity at least one month in a year (Mesfin & Arjen, 2016). At present, there are a variety of commonly research methods of water resources stress, which can be divided into four categories according to the calculation principle: single index method, supply-demand ratio method, comprehensive evaluation method, and water footprint assessment method. Falkenmark originally proposed a gross per capita freshwater demand, defining it as the water stress index (WSI), with water stress occurring when per capita water demand falls below 1700 m3/a (Falkenmark et al., 1989). The Falkenmark index (FI) is straightforward to calculate but overlooks the critical role of demand, which is linked to economic and societal factors. The supply-demand ratio method, which analyzes water stress from a supply-demand perspective, defines the water stress index as the ratio of total water removal to total available water. This method has been used by some scholars to evaluate global water resource pressure with the Water Gap model, and its results have been widely applied in the study of global water scarcity (Raskin, 1997; Cosgrove et al., 2000). While the supply-demand ratio method is intuitive, data acquisition and calculation method are straightforward, and the evaluation is accurate, its application in China is limited. The comprehensive evaluation method employs multiple indexes and perspectives to assess water stress induced by human activities. However, this approach demands extensive data and lacks consistency in index selection and weight allocation, making it less effective in reflecting regional characteristics (Sullivan, 2002; Wang et al., 2007). The water footprint assessment has gained international recognition and application, but it still fails to capture the regional nuances of water resource pressure and does not adequately consider ecological water requirement (Jia et al., 2016). The contradiction between water resource supply and demand in Southern Xinjiang accentuates water stress. Given the anticipated changes in water resources due to climate change and human activities, there is an urgent need for a simple and consistent method to comprehensively assess the current and future water stress in the region.

This study employed a monthly-scale degree-day model to simulate glacial meltwater volume in the basin, combining it with precipitation trends to predict future water supply in the study area. Population and economic development trends in the region were used to forecast future water resource demand. By considering water supply and demand, we calculated the water stress index using the supply-demand ratio method, enabling the assessment of historical and future water stress in the three regions of Southern Xinjiang. The Morlet wave was employed to analyze precipitation cycle in these regions. This study unveils the spatiotemporal variations in water resources imbalance in the regions, offering valuable scientific insights for water resources management and rational utilization in Southern Xinjiang.

2 Materials and Methods

2.1 Research area

Southern Xinjiang is deep in the hinterland of Eurasia and surrounded by high mountains. The average elevation of the mountains is 4000~6000 m, and the highest point is 8611 m. The high mountains hinder the entry of warm and humid air from the southeast and southwest monsoons, changing atmospheric circulation and making the area windy and dry, while the mid-

latitude effect creates less precipitation (50~70 mm) and strong evaporation (1125~1600 mm). At the same time, tall mountain peaks provide favorable hydrothermal conditions for glacier development, and glaciers covering 5,000-6,500 m above sea level account for 70% of the glacier area in the entire basin (Shangguan, 2007). The Aksu, Kashgar and Hotan areas are the three main administrative regions in the Tarim River Basin in southern Xinjiang (referred to as the three regions in southern Xinjiang, or TRSX, the same below, Figure 1). The Aksu, Weigan, Yarkant, Hotan and Kriya Rivers, which originate from the alpine glaciers on the edge of the Tarim Basin, are distributed in these three regions. Meltwater runoff accounts for 30.8%~69.0% of the total runoff. Among these five rivers, Aksu River and Weigan River are located in Aksu region, Yarkant River in Kashgar region, Hotan River and Keriya River in Hotan region.

The TRSX have a land area of 542,300 km^2, accounting for approximately one-third of Xinjiang's land area. It includes typical ecologically fragile areas dominated by agriculture. As of 2020, the total population was 9.17 million, the rural population accounted for 78.53%, and the total output value of the primary industry was 153.68-billion-yuan, accounting for 52.77% of the total output value. Agriculture is an important support for TRSX economic development. Agricultural water accounts for more than 90% of the total water use, and the amount of water resources developed and utilized in the entire southern Xinjiang region has exceeded 95% of the available amount, which is much higher than the international level. By convention, the water resource development rate of inland, arid rivers does not exceed 70%, and water resources in southern Xinjiang are in a state of overexploitation. In recent years, with the melting of glaciers, the water resources are increasing. At the same time, the water demands in TRSX are sharply increasing, with agricultural water use increasing for the rapid expansion of oases and arable land, and domestic and industrial water demand increasing for economic development and population growth. As a result, the contradiction between the supply and demand of water resources has become increasingly prominent, and the region will face more severe water shortages.

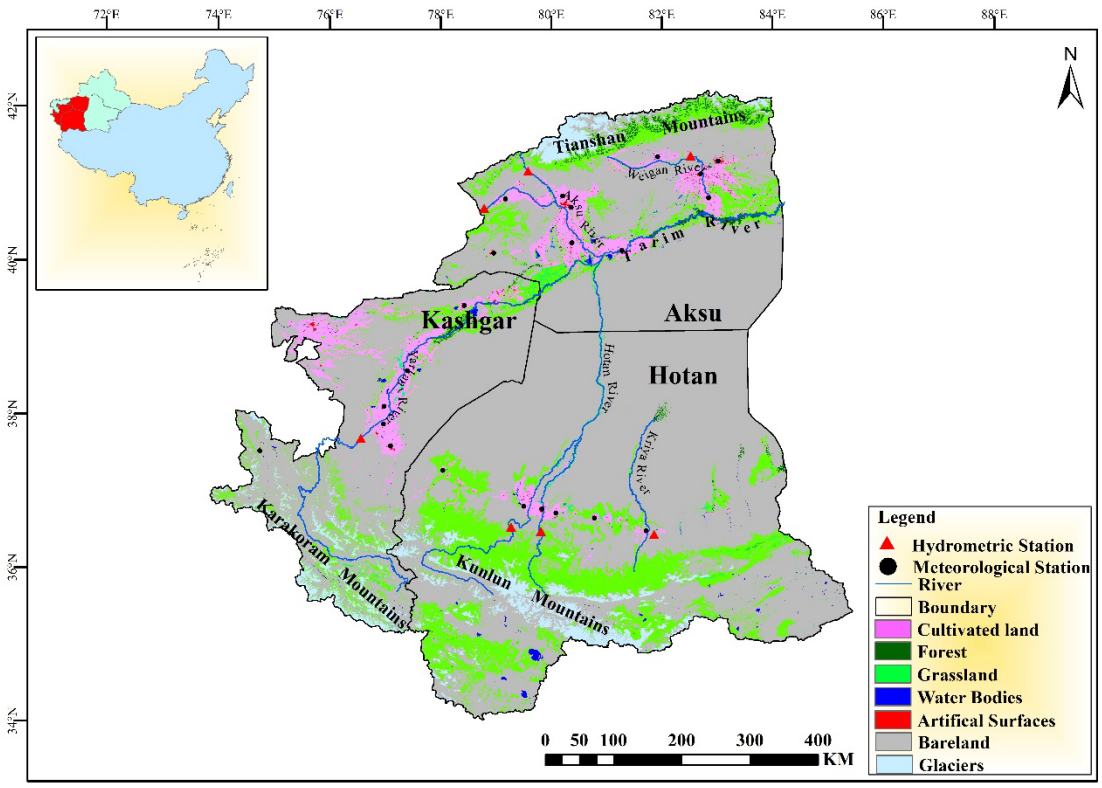

Fig1 Diagram of the study area

2.2 Data sources

(1) Socio-economic data. Data on population, gross industrial output, number of livestock and total water resources in 2000, 2010 and 2018 were obtained from the Xinjiang Statistical Yearbook. Water quota of domestic, industrial output value and livestock refer to the water quota standards formulated in the "*Notice on Printing and Distributing Industrial and Domestic Water Quotas in Xinjiang Uygur Autonomous Region*". Population, gross industrial output, number of livestock and crop acreage were forecasted according to the white paper "*Population Development in Xinjiang*" and the "*14th Five-Year Plan for National Economic and Social Development in Each Region and Outline of Vision 2035*".

(2) Meteorological data. Data from 16 meteorological stations in the study area were selected, including daily maximum temperature, average temperature, daily minimum temperature, humidity, wind speed, sunshine hours and precipitation. The data came from the National Meteorological Science Data Center (http://data.cma.cn/) and the Resource and Environment Science and Data Center (http://www.resdc.cn/). The climate data outputs from Phase 6 of the Coupled Model Intercomparison Project (CMIP6) GCMs, under the SSP2-4.5 (moderate radiation forcing scenario) and SSP5-8.5 (high radiation forcing scenario) scenarios, were used to project the response of hydrological processes to future climate change.

(3) Phenological data. The growth periods and crop coefficients of the main crops in the study area were recommended by the United Nations Food and Agriculture Organization (FAO).

(4) Land-use data. Oasis land use data were extracted based on remote sensing images from 2000, 2010 and 2018 provided by the Geospatial Data Cloud (https://www.gscloud.cn), the 30 m global surface coverage is provided by the National Catalogue Service for Geographic Information (https://www.webmap.cn).

2.3 Estimating oasis's available water resources

2.3.1 Evaluating Glacier Meltwater

Degree-day factor model is one of the most commonly used methods to estimate glacier mass balance and its response to climate change. Studies have shown that the degree-day model can better simulate the mass balance and meltwater at the catchment scale (Gao *et al.*, 2010; Zhang *et al.*, 2012).

(1) Degree-day model

The magnitude of oasis runoff in southern Xinjiang is mainly related to the melting of ice and snow (Zhang, 2008). Therefore, this study used a degree-day model to better simulate meltwater runoff at the watershed scale. For ice and snow, the mass balance model was calculated as follows:

$$A = DDF \times PDD \quad (1)$$

where A is the melting water equivalent of snow and ice in a certain period of time (mm); DDF is the degree-day factor of ice or snow (mm/d °C); and PPD is the positive accumulated temperature in the same period of time, obtained from the following formula:

$$PDD = \sum_{i=1}^{n} Ht \cdot Tt \quad (2)$$

where n is the number of days in the month, $i = 1$ refers to the calculation from the 1st day of each month; T_t is the daily average temperature (°C) of a given day, H_t is a logical variable, when $T_t \geq 0$ °C, $H_t = 1$, when $T_t < 0$°C, $H_t = 0$.

$$B_n = P - A \quad (3)$$

where B_n is the mass balance of the glacier over a given period of time (mm), and P is the solid precipitation (mm) in the glacier area over a given period of time. The glacier meltwater in the basin is calculated as follows:

$$Q = \sum_{j=1}^{n} s(j)[(1-f)A(j) + P_{liq}(j)] \quad (4)$$

where Q is glaciers meltwater in the basin; $s(j)$ for the area of the jth elevation band; f is the refreeze ratio; $P_{liq}(j)$ for the liquid precipitation of the jth elevation band.

Firstly, the monthly precipitation and temperature data of the glacier end height are interpolated by using the measured data of the meteorological stations. Secondly, the monthly temperature and precipitation in each elevation zone are generated by using the temperature decline rate and precipitation gradient. Then, according to the degree-day model, the glacier mass balance and meltwater runoff are output, the total glacier meltwater runoff is obtained from the meltwater runoff and area of each elevation zone. Finally, the mountain discharge in the basin is calculated by the proportion of glacier meltwater in the total runoff in each region. The calibration of the model parameters is based on the comparison between the simulation results of

the model and the short-term observation data in the same period of time and the previous glacier meltwater research results.

(2) Model parameters

The glacier area in each elevation zone was generated at 100 m intervals according to the glacier vector map and DEM in the basin. Elevation bands were independently of each other.

At the glacier scale, due to the scarcity of measured data, the degree-day factor value was generally calibrated based on observation data for typical glaciers and then extended to surrounding glaciers. This study referred to degree-day factor values from existing research (Zhang, *et al*., 2019) and then compared the simulated glacier mass balance and meltwater runoff with the data. Then, the average degree-day factor for each watershed was adjusted and determined (Table 1).

Tab1. Degree-day factor coefficients of eac

Basin	Aksu	Weigan	Yarkant	Hotan	Kriya
Ice	2.50	2.20	7.30	8.80	11.00
Snow	1.40	1.50	4.50	5.40	7.00

Temperature and precipitation data of glacier base were obtained by interpolating the measured data from the national meteorological stations in the basin. Temperature and precipitation gradients were based on previous research data (Gao, *et al*., 2010), and then the temperature and precipitation data in each elevation band were obtained. Although the meteorological data obtained by interpolation may not be accurate enough to correspond to the specific location, because the final calculation was glacier meltwater at the watershed scale, it was necessary only to be as reasonable as possible at that scale.

The critical temperature of solid precipitation in each basin (T_s = -0.5 °C), the critical temperature of liquid precipitation (T_l = 2 °C), solid precipitation correction factor (1.3), liquid precipitation correction factor (1.1), and meltwater refreeze ratio (f = 0.2), were based on the existing research (Gao *et al*., 2010; Zhang *et al*., 2012).

(3) Model verification

Because there are no measured data at the watershed scale in the study area, the simulated mass balance and glacier meltwater were indirectly verified by comparison with other results from the literature. It is mainly carried out from two aspects of glacier mass balance and glacier meltwater:

Glacier mass balance. The simulated results show that the average annual mass balance of the glaciers in Yarkant River Basin during 1961-1990 is -122.77 mm, and the result of Gao during the same period is -117.50 mm (Gao *et al*., 2010), Kang *et al.* estimated that the average annual mass balance of glaciers in Yarkant River Basin is -100.10 mm during 1951-1990 by using the maximum entropy principle (Kang et al., 2002). During 1961-2000, the simulated annual glacier mass balance in Yarkant River Basin was 158.30 mm, while Shen *et al.* estimated that mass balance in the Pamir and Karakoram Mountains was about -150.00 mm at the same

period (Shen et al., 2002). After 1991, the mass loss became more significant, and the average annual mass balance reached -320.10 mm, the estimated value of other studies was -301.20 mm in the same period (Gao et al., 2010).

Glacier meltwater runoff. The average annual glacier meltwater runoff of the five basins simulated by the degree-day model from 1961 to 2000 was 117.27×10^8 m^3, while that of the Tarim River basin estimated by other studies was 138.72×10^8 m^3 (Gao *et al*., 2010). The annual average glacier meltwater runoff from 2000 to 2010 was 129.94×10^8 m^3 in this study, while the other studies' value was 133.42×10^8 m^3 in 2000 and 126.54×10^8 m^3 in 2004 respectively (Kang *et al*., 2002; Xie *et al*., 2006). The model simulated the glacial meltwater runoff for the five major river basins of the Aksu, Weigan, Yarkant, Hotan and Kriya Rivers. The comparison data were glacial meltwater runoff for the entire Tarim River basin, so the simulated values were less than reported results.

In addition, according to the glacier area-volume relationship of China's measured data, the revised formula for volume calculation proposed by Liu is applied to verify the simulation data (Liu, et al., 2003).

$$V = 0.04S^{1.35} \quad (5)$$

where V is the glacier volume （km^3）; S is the glacier area （km^2）.

According to the glacier area of the first (1999) and second (2014) glacier inventory, the changes of glacier volume in each basin are calculated. According to the formula, the glacier volume in Aksu River Basin, Weigan River Basin, Yeerqiang River Basin, Hotan River Basin and Keliya River Basin decreased by812×10^8 m^3, 139×10^8 m^3, 788×10^8 m^3, 454×10^8 m^3 and 89.2×10^8 m^3, respectively, equivalent to an average annual water equivalent of 45.98×10^8 m^3, 7.89×10^8 m^3, 44.66×10^8 m^3, 25.75×10^8 m^3, and 5.06×10^8 m^3. In this study, the average annual glacial meltwater simulated by the model is 45.74×10^8 m^3, 7.69×10^8 m^3, 47.89×10^8 m^3, 27.59×10^8 m^3 and 4.98×10^8 m^3 respectively.

From the results of the above comparison and verification, the simulation results of this model are in good agreement with the other studies and the calculation results of the revised formula for volume, which can simulate glacier mass balance and meltwater runoff with high reliability.

2.3.2 Calculation method of available water resources

Precipitation is scarce in the oases of southern Xinjiang, and water resources mainly come from surface runoff formed by glacial meltwater and precipitation in mountainous areas. Therefore, in this study, the amount of incoming water from the mountain area (that is, the flow out of the mountain) minus the amount of unusable surface water was taken as the amount of water resources available to the oases.

$$W_S = （W_R - W_{UN}） \times \theta\% \quad (6)$$

where, W_S is the amount of water resources available for oases development (10^8 m^3); W_R is the flow out of the mountain (10^8 m^3); W_{UN} is the amount of surface water that cannot be used (10^8 m^3), which is mainly the amount of water that each source must provide for ecosystem stability in the main stream of the Tarim River (Chen *et al*, 2013), $\theta\%$ for the utilization of water resources (2018 Xinjiang Water Resources Bulletin).

2.4 Estimating oasis water demand

The development of southern Xinjiang is constrained by water resources, so building a complete water demand system will help measure actual water consumption more accurately. Water use in southern Xinjiang is mainly divided into main aspects: domestic water demand, production water demand and ecological water demand, as shown in Equations (7) and (8).

$$W_T = W_D + W_P + W_E \tag{7}$$

$$W_P = W_I + W_G + W_A \tag{8}$$

where W_T represents the total water demand; W_D, and W_E represent domestic (DWD) and ecological (EWD) water demand, respectively; and W_I, W_G and W_A represent industrial water demand (IWD), livestock water demand (LWD) and agricultural water demand (AWD), respectively. The unit is $10^8 m^3$.

In the above water demand system, the DWD, IWD and LWD were calculated based on the water quota method, and the total water demand of each department was calculated according to the "Xinjiang Industrial and Domestic Water Quota Standard", as shown in Equations (9, 10, 11).

$$W_L = Q_C \times P_C + Q_R \times P_R \tag{9}$$

$$W_I = Q_I \times V_I \tag{10}$$

$$W_G = Q_B \times M_B + Q_S \times M_S \tag{11}$$

where, Q_C and Q_R represent the urban and rural residents' domestic water quotas, respectively (L/person/day); P_C and P_R represent the number of urban and rural residents, respectively (person); Q_I is the water consumption per ten thousand yuan of industrial added value ($m^3/10^4$ yuan); V_I is the industrial added value (10^4 yuan); Q_B and Q_S represent the water demand quotas of large and small livestock (L/head/day); and M_B and M_S represent the number of large and small livestock (heads), respectively.

Vegetation EWD was determined based on shallow groundwater evaporating, a method that is widely applied in arid areas. After summarizing the previous studies on EWD in arid areas, this study uses the phreatic evaporation method to calculate vegetation EWD in each region, as shown in Equations (12, 13).

$$W_E = \sum A_i W_{gi} K_p \tag{12}$$

$$W_{gi} = a(1 - H/H_{max})^b \times ET_{\emptyset 20} \tag{13}$$

where, A is the vegetation area (m^2);W_{gi} is the submersible evaporation (mm);K_p is the vegetation coefficient; H is the optimum groundwater depth for vegetation (m);H_{max} is the limit depth of groundwater evaporation (m) ;$ET_{\emptyset 20}$ is the evaporation value of the water surface of the 20 cm diameter evaporating dish (mm); *a* and *b* are the empirical coefficients, which are related to the soil texture. The phreatic evaporation of different soil qualities differs across desert areas and the values of empirical coefficients *a* and *b* were 0.62 and 2.8, respectively. According to the existing research, the limit depth of groundwater evaporation and the average depth of each vegetation type were determined in southern Xinjiang (Cao *et al.*, 2012). $ET_{\emptyset 20}$ values were obtained on observation data from regional meteorological stations, and were 1973.4 mm in the Aksu region, 2450.5 mm in the Kashgar region, and 2607.2 mm in the Hotan region.

The evapotranspiration of crops directly affects crops water demand. Reference crop evapotranspiration ET_0 characterizes the impact of meteorological factors on crop water requirements and then combines crop coefficients to determine crop evapotranspiration ET_c in different growth periods. For this study, ET_0 Calculator software developed by the United Nations FAO was used to calculate ET_0.

$$ET_{ci} = K_{ci} \times ET_{0i} \quad (14)$$

$$W_A = \sum A_i \times ET_{ci} \quad (15)$$

where, ET_{ci} is the evapotranspiration of crop i (mm); ET_{0i} is the reference crop evapotranspiration (mm) in the same period as the growth period of crop i; K_{ci} is the crop coefficient of crop i; and A_i is the planting area of crop i (m^2). By consulting the Statistical Yearbook, it was found that the main crops in southern Xinjiang were wheat, maize, cotton and rice. The crop coefficient referred to the recommended FAO value and existing research in southern Xinjiang (Lv *et al.*, 2017).

2.5 Oasis water security analysis

Water scarcity is an obvious risk factor for water systems and causes significant losses globally. Existing water scarcity risk analyses have mainly focused on the relationship between water supply and demand without considering the high-low cycle of regional precipitation. Furthermore, consecutive periods of water scarcity are certainly a greater risk than situations where periods of shortage are separated by periods of sufficient supply, and the length of consecutive dry years should be considered as part of a risk analysis. Therefore, this study considered regional water resource scarcity in a comprehensive way——water stress index, the regional precipitation cycle, and the length of the wet-dry years to analyze the current and future water security risks in the TRSX.

2.5.1 Water stress index (WSI)

Water stress will occur when water resources are short or existing water resources cannot meet the needs of human society and natural environment (Damkjaer & Taylor, 2017). In this paper, the water stress index (WSI) is defined as the ratio of total water demand to total available water (Alcamo, et al., 1999).

$$WSI = \frac{W}{Q} \quad (16)$$

where WSI is water stress index; W is the total water demand, including domestic water, industrial water, livestock water, agricultural water and ecological water（m^3）; Q is the total available water（m^3）. Refer to the table2 for specific indicators.

Tab2. WSI Indicators

Range	WSI≤0.1	0.1<WSI≤0.2	0.2<WSI≤0.4	0.4<WSI≤0.7	WSI>0.7
	Surplus	Slight shortage	Moderate shortage	Severe shortage	Awful shortage

2.5.2 Analysis of high-low precipitation

The annual precipitation is uncertain and can have a very large adverse impact on the utilization of water resources. Precipitation variability significantly affects water resources regulation and planning. Wet and dry years were divided according to the following criteria (Zhang, 2008):

Plentiful Year: $P_i > \overline{P_N} + 0.33\sigma$; dry years: $P_i > \overline{P_N} - 0.33\sigma$

where $\overline{P_N}$ is the average annual precipitation; sP_i is the annual precipitation; and σ is the mean variance.

For a specific watershed, the variation cycle of precipitation abundance and dryness has some regularity. By decomposing the time series into the time-frequency domain, the wavelet transform obtains the time series significant fluctuation pattern, or the cycle transforms dynamics (Ling et al., 2013, Torrence et al., 1998). The choice of wavelet function depends on specific signal. The Morlet wavelet function$\Psi(t)$ is often used in the field of climate and hydrology, and is represented by the following expression:

$$\Psi(t) = \pi^{-1/4} e^{ict} e^{-t^2/2} \tag{17}$$

where i is an imaginary unit, t is a dimensionless time parameter, and c is a constant.

A continuous wavelet transformation of a discrete signals$f(t)$ with a Morlet wavelet$\Psi(t)$ is:

$$W_f(a,b) = \frac{1}{a}\int_R f(t)\Psi^*(\frac{t-b}{a})\,dt \tag{18}$$

In the formula, $W_f(a,b)$ is the wavelet transform coefficient, the value obtained from the continuous wavelet transform. It indicates the degree of approximation between part of the signal and the wavelet; a is the scale parameter, b is a translation parameter, t for time, and $\Psi*$ represents the complex conjugate.

The real part coefficients and mode are two very important variables in the wavelet transform coefficient graph. The real part coefficients represent the phase distribution of time-scale signals with different features at different times, meaning that they represent the change in abundance and dryness of the hydrological series. The closed center of the contour line represents the change center of the precipitation series, and the positive value of the contour line indicates that the precipitation was more abundant. Negative values indicate that the precipitation was relatively low, and when the wavelet transform coefficient was zero, it corresponded to the mutation point of the sequence. The mode indicated the magnitude of the characteristic time scale signal.

The wavelet variance determined the main period of precipitation in the time series, and the peak value was the main change period. The expression is written as follows:

$$\boldsymbol{Var(a)} = \int_{-\infty}^{+\infty} |\, W_f(a,b)\,|^2\, db \tag{19}$$

3 3 Results and Analysis

3.1 Analysis on the present situation of water resources in TRSX

Utilizing meteorological and runoff data, we have conducted an analysis of the changes in water resources in five river basins in TRSX over the past 60 years. Runoff recharge in

Southern Xinjiang is comprised of three main components: precipitation, alpine glacier meltwater, and groundwater. As presented in Table 3 and Figure 2, the runoff generated by precipitation and glacial meltwater, as well as the total runoff in the five major river basin, exhibit an overall upward trend. However, the rate of increase and its statistical significance vary.

Precipitation in southern Xinjiang has generally increased due to global warming. The runoff formed by precipitation has ranged from $1.09\times10^8 m^3/a$ to $20.28\times10^8 m^3/a$， but the trend and significance have not been consistent across all river basins. Aksu, Weigan and Yarkant River Basins have experienced relatively significant increase in precipitation with slopes of 0.19 mm/a, 0.03 mm/a and 0.12 mm/a, respectively, passing significance tests at the 0.01 level. The Hotan River Basin has shown a slower increase in precipitation compared to Aksu and Yarkant, with a slope of 0.08mm/a, passing the significance test at the 0.05 level. Meanwhile, the Kriya River Basin exhibited the slowest growth with a slope of 0.01 mm/a, failing to pass the significance test at the 0.1 level. This indicates that the average growth rate of precipitation runoff in the western part of southern Xinjiang (Aksu, Yarkant and Hotan River basins) has been greater than that in the eastern part (Weigan and Kriya River basins).

Glacier meltwater is a crucial water resource in TRSX. Recent years have witnessed significant changes in glacier meltwater due to global warming and rising temperature. The accumulated mater balance in Aksu River Basin and Weigan River Basin, originating from Tianshan Mountain, is negative at -17.5m and -12.4m, respectively, with annual average increases in meltwater of $(0.10 \pm 0.07) \times 10^8 m^3/a$ ($P > 0.1$) and $(0.04 \pm 0.01) \times 10^8 m^3/a$ ($P < 0.01$). The glacier area in Aksu River Basin has decreased by $403.33 km^2$, with a shrinking rate of -0.44%/a, while that in Weigan River Basin has decreased by $127.08 km^2$, with a shrinking rate of-0.2%/a. Yarkant River Basin has also suffered substantial material loss, with a cumulative material balance of -14.2m, annual average meltwater increases of $(0.06 \pm 0.09) \times 10^8 m^3/a$ ($P > 0.1$), glacier area reduction by $927 km^2$, and a recession rate of -0.36%/a. The Hotan and Kriya River Basins, originating from Kunlun Mountain, which has the largest number of glaciers in western China, are characterized by large-scale glaciers. Despite temperature-induced shrinkage, the total area has decreased by approximately 7%, maintaining overall stability. Prior to 1990, glaciers in the Hotan and Kriya River Basins were generally in a positive material balance, with slight accumulation. However, after 1990, they experienced material losses. The annual average increase of meltwater is $(0.05\pm0.06) \times 10^8 m^3/a$ ($P > 0.1$) and $(0.02\pm 0.01) \times 10^8 m^3/a$ ($P < 0.05$), with shrinkage rates of -0.36%/a and -0.095%/a, respectively. The average growth rate of glacial meltwater runoff in the western region (Aksu, Yarkant and Hotan River basins) has exceeded that in the eastern region (Weigan and Kriya River basins).

With both precipitation and glacier meltwater on the rise, the runoff in the five major river basins in southern Xinjiang is showing an increasing trend. The annual runoff for Aksu, Weigan, Yarkant, Hotan and Kriya Rivers is （0.38±0.07）$\times10^8 m^3/a$（P<0.01）, （0.14±0.03）$\times10^8 m^3/a$（P<0.01）, （0.23±0.09）$\times10^8 m^3/a$（P<0.05）, （0.17±0.07）$\times10^8 m^3/a$（P<0.05）, and（0.04±0.01）$\times10^8 m^3/a$（P<0.01） respectively. This indicates that the average growth rate of total runoff in the western region (Aksu, Yarkant and Hotan River basins) was greater than that in the eastern region (Weigan and Keliya River basins).

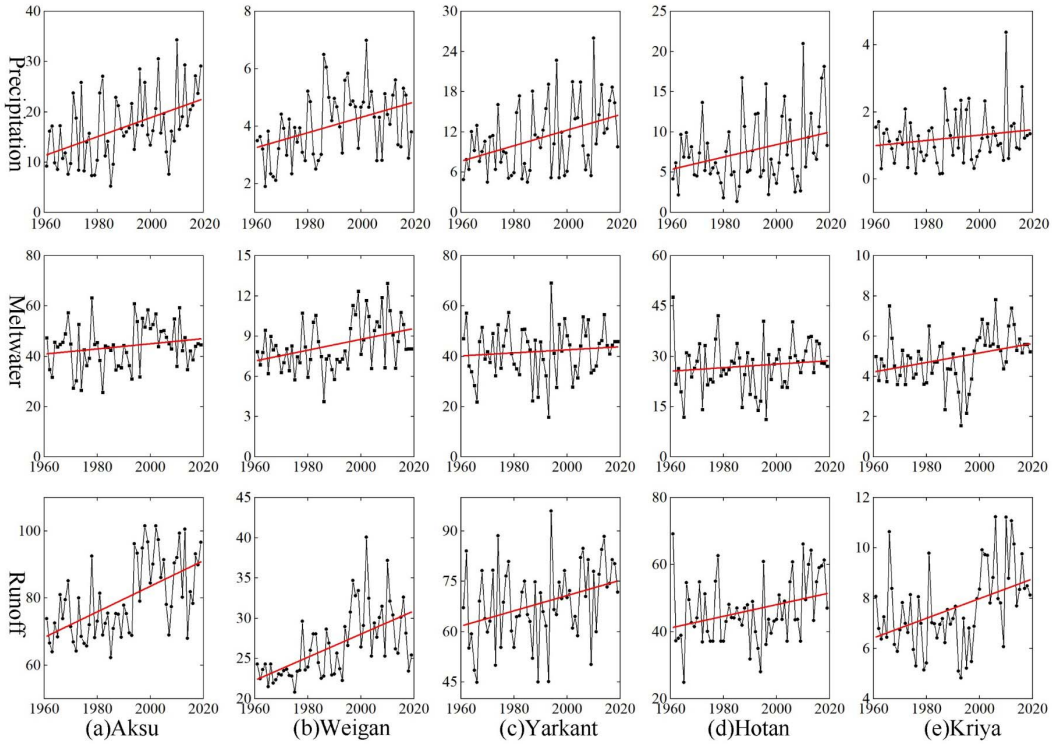

Fig2. The change trend of precipitation, meltwater and runoff in five basins in southern Xinjiang from 1960 to 2020

Table3 Annual averages and changes of precipitation, glacial meltwater and runoff in southern Xinjiang from 1960 to 2020

	Basin	Average annual water ($10^8m^3/a$)	sd	Change ($10^8m^3/a$)	sd
Precipitation	Aksu	20.28	9.17	0.19***	0.05
	Weigan	2.37	0.70	0.03***	0.01
	Yarkant	11.01	7.06	0.12***	0.04
	Hotan	10.41	6.45	0.08**	0.03
	Kriya	1.09	0.68	0.01	0.01
Glacier	Aksu	39.99	10.61	0.10	0.07
meltwater	Weigan	9.95	1.82	0.04***	0.01
	Yarkant	42.03	12.29	0.06	0.09
	Hotan	23.95	8.86	0.05	0.06
	Kriya	4.98	1.24	0.02**	0.01
Runoff	Aksu	78.99	11.32	0.38***	0.07
	Weigan	26.45	4.22	0.14***	0.03
	Yarkant	68.53	12.30	0.23**	0.09
	Hotan	45.81	9.46	0.17**	0.07
	Kriya	7.49	1.61	0.04***	0.01

Note: * is represented as P<0.1, ** as P<0.05, *** as P<0.01, sd as standard deviation.

3.2 Analysis of precipitation change cycle

Understanding the variability of precipitation can provide valuable insights for the scientific management of water resources. Therefore, we conducted anomaly processing on the annual average precipitation in the study area over the past 60 years and applied the Morlet wavelet for continuous wavelet transform on the precipitation anomaly sequence. This allowed

us to identify variability cycles of precipitation at different time scales in the study area, with the main change periods represented by the peak wavelet variance.

The contour map of the real part of the Morlet wavelet transform shows annual average precipitation variability at different time scales. Among them, the red part represents the wet season with more precipitation, and the blue part represents the dry season with less precipitation. The wavelet variance peak indicates the main change period.

The time-frequency diagram of the real part of the wavelet transforms coefficients (Figure. 3a-c) shows that the energy-frequency domain scales in the Aksu region were primarily concentrated within 7-15 years and 30-45 years, while in the Kashgar region, they were 0-5years and 5-15years. In the Hotan region, they were 5-15years and 40~50years. Additionally, when calculating the wavelet variance of the entire time series, the highest and second-highest peaks were observed at scales of 11 years and 38years in the Aksu region, 12 years and 4years in the Kashgar region, and 12 years and 44 years in the Hotan region, indicating the strongest periodic oscillations at these scales (Figure. 3d-f).

To further analyze the precipitation changes, we plotted the change process curve of the real part of the wavelet coefficient at the corresponding period scale of the time series (Figure. 4). Over the past 60 years, all three regions experienced the most significant fluctuations at the scales of 11 years, 12 years and 12 years, with clear cyclical changes emerging after 1975. Specifically, the Aksu region witnessed seven high-low alternations at the 11 years scale, with an average cycle of 8 years. The Kashgar region experienced seven complete high-low cycles at the 12 years scale, averaging an 8 years cycle, while the Hotan region wxhibited a similar pattern to Kashgar.

By applying the classification standard of wet and dry years, we identified consecutive wet and dry seasons lasting for more than two years (including 2 years) in the three regions (Table 4). In the past 60 years, the Aksu, Kashgar and Hotan regions experienced 5, 6, and 6 consecutive dry seasons, respectively, with a maximum of 4, 4, and 5 consecutive years, respectively.

498 Table 4. Statistical table of the consecutive wet and dry years in the TRSX

	Wet season		Dry year	
	Start-end year	Number of years	Start-end year	Number of years
Aksu	1981~1982	2	1961~1962	2
	1987~1989	3	1964~1965	2
	1991~1993	3	1967~1970	3
	1995~1996	2	1978~1980	3
	2001~2003	3	1983~1986	4
	2015~2019	5		
Kshgar	1981~1982	2	1961~1963	2
	1992~1993	2	1969~1970	2
	2002~2005	4	1978~1980	3
	2012~2013	2	1983~1986	4
	2016~2018	3	1999~2000	2
			2007~2009	3
Hotan	1987~1988	2	1969~1971	3
	2002~2003	2	1975~1976	2
	2012~2013	2	1978~1980	3
	2016~2018	3	1983~1986	4
			1997~2001	5
			2007~2009	3

499

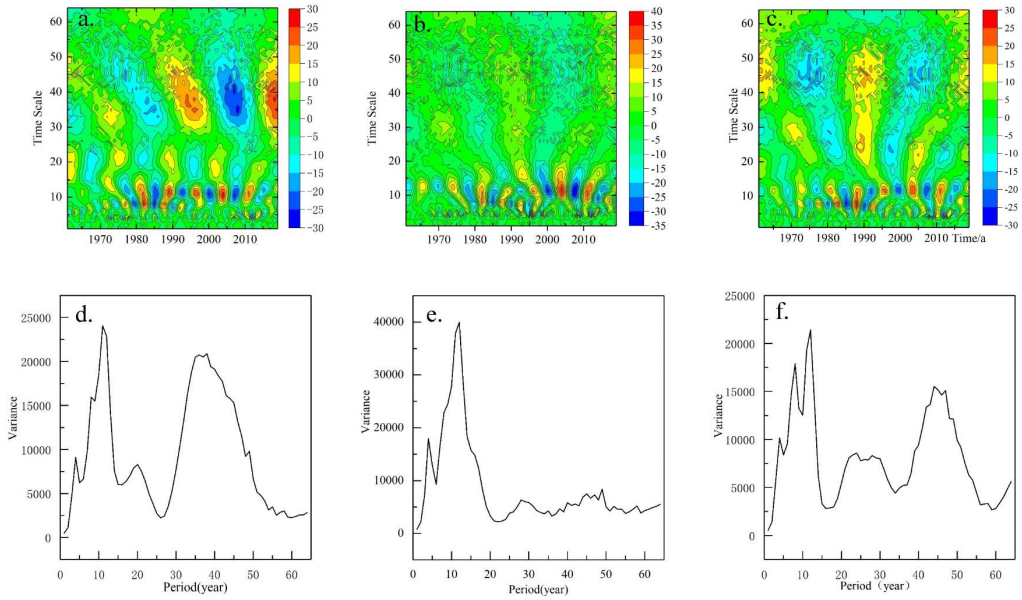

Figure 3. Real part contour map of wavelet transforms coefficients: (a) Aksu area; (b) Kashi area; (c) Hotan area; wavelet variance: (d) Aksu area; (e) Kashi area; (f) Hotan area

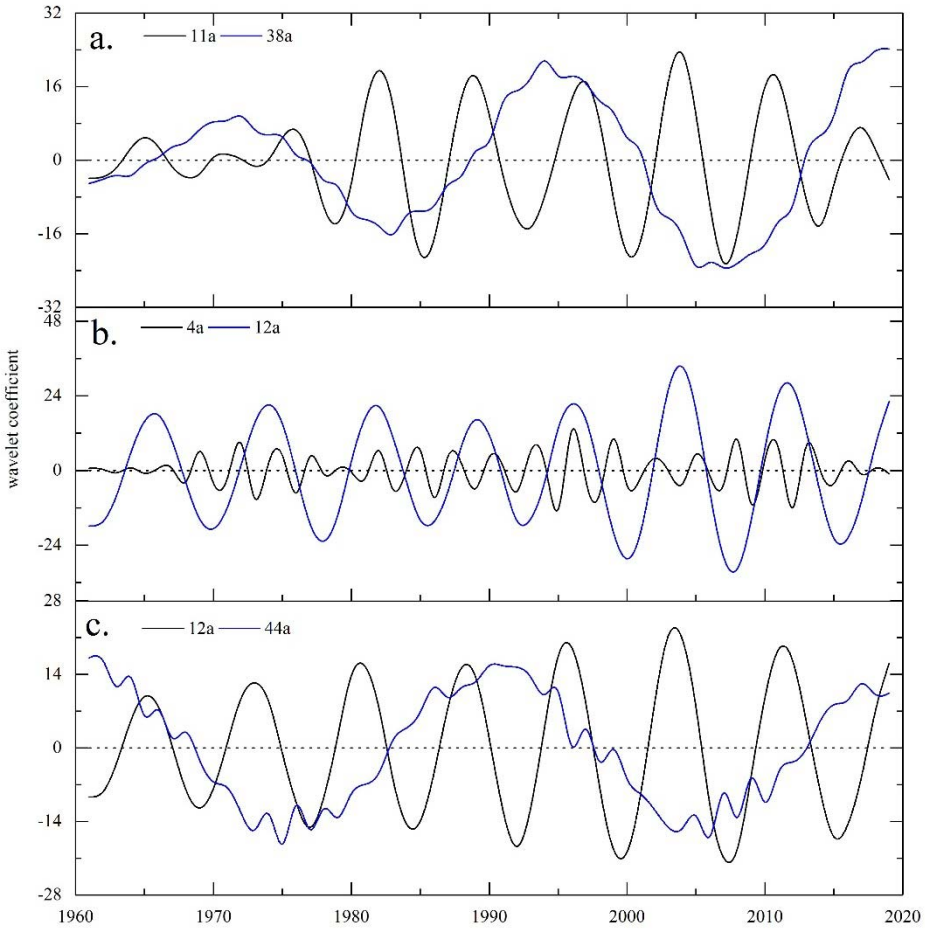

Figure 4. Wavelet Coefficient Real Part Transform Curve

3.3 Analysis of the present situation of water demand in TRSX

The development of oases in arid regions is impeded by limitations associated with water resources. Utilizing meteorological data, land use data, and socio-economic data, the study conducted an evaluation of domestic water demand (DWD), industrial water demand (IWD), livestock water demand (LWD), agricultural water demand(AWD) and ecological water demand (EWD) within TRSX over the past two decades. The outcomes, as depicted in Table 5 and Figure5, reveal a noteworthy upward in water consumption across various sectors within TRSX.

Table5 Annual averages and changes of DWD, IWD, LWD, AWD and EWD in southern Xinjiang from 2000 to 2020

	Region	Average annual water（$10^8m^3/a$）	sd	Changes （$10^8m^3/a$）	sd
DWD	Aksu	0.80	0.31	0.05***	0.01
	Kashgar	1.27	0.52	0.08***	0.01
	Hotan	0.63	0.28	0.04***	0.00
IWD	Aksu	1.22	0.88	0.13***	0.01
	Kashgar	1.06	0.70	0.11***	0.01
	Hotan	0.27	0.17	0.03***	0.00
LWD	Aksu	0.76	0.09	0.01***	0.00
	Kashgar	1.11	0.11	0.00	0.00
	Hotan	0.67	0.07	0.01	0.00
AWD	Aksu	40.12	14.96	2.32***	0.20
	Kashgar	46.20	15.49	2.19***	0.31
	Hotan	11.56	1.43	0.02**	0.01
EWD	Aksu	7.50	1.19	-0.16**	0.04
	Kashgar	8.75	1.39	0.12*	0.09
	Hotan	8.24	1.72	-0.21*	0.07

Note: * is represented as P<0.1, ** as P<0.05, *** as P<0.01, sd as standard deviation.

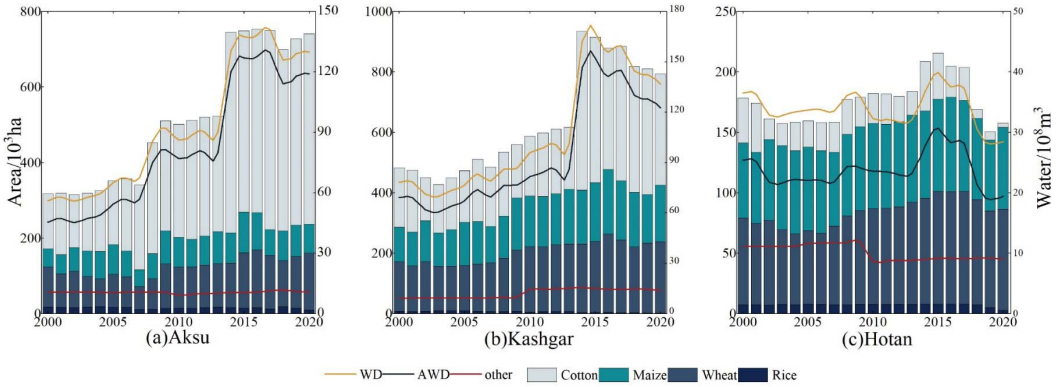

Fig5. Area of main crops and water demands of TRSX

Table 6 illustrates that artificial oases have experienced substantial expansion in the last two decades. Consequently, both DWD and IWD in TRSX exhibited a marked increase trend ($P<0.01$). Notably, the Kashgar region offering the highest population, also records the most substantial annual DWD, coupled with the most considerable annual increase. The Hotan region exhibits the fastest increase [(0.67%±0.38%), $P<0.01$], followed by the Kashgar region [(0.41%±0.22%), $P<0.01$], while the Aksu region demonstrates the slowest increase [(0.37%±0.21%), $P<0.01$]. Disparities in average annual IWD in TRSX were discernible. Comparatively, Aksu and Kashgar regions exhibited minimal divergence, with similar average annual increments. In contrast, Hotan region, characterized by less advanced industrial development, reported lower IWD levels, accompanied by a notably lower average annual increase, relative to the other two regions. The LWD within TRSX remained relatively stable, with a growth rate falling below $0.01\times10^8 m^3/a$.

526 Tab6. Status of the study area from 2000 to 2018 (km^2)

Region	Year	Cultivated land	Artificial oasis	Natural oasis	Oasis
Aksu	2000	3539.00	9947.2	23756.96	33704.16
	2010	6149.40	13750.66	16859.64	30610.29
	2018	6593.70	16270.62	15010.90	31281.52
Kshgar	2000	4077.10	10362.94	15454.90	26418.97
	2010	5304.60	12800.37	13809.38	27163.31
	2018	7099.60	15073.45	11957.48	27518.46
Hotan	2000	1728.60	2629.79	22546.63	25176.42
	2010	1726.20	3419.23	13698.43	17117.66
	2018	2264.60	4205.73	13282.12	17487.85

527 In southern Xinjiang, agricultural water represents the predominant sector in water
528 consumption, accounting for over 70%~90% of total regional water usage. Table6 reveals a
529 substantial increase in cultivated land wihin TRSX, witnessing growth rates of 86.32%, 74.13%,
530 and 31.01% from 2000 to 2018, respectively. This alteration in cultivated land directly
531 influenced the utilization of agricultural water. AWD within the Aksu and Kashgar regions
532 registered sharp increases, while in the Hotan region, it remained relatively stable with a minor
533 decrease. Over the past two decades, AWD escalated by 162.89% in the Aksu region, 88.08% in
534 the Kashgar region, and 23.46% in the Hotan region. The incongruent alterations in AWD
535 among these three regions are attributable to varying adjustments in the planting areas of major
536 crops (Figure 5). Specifically, expansive cotton in the Aksu and Kashgar regions triggered a
537 substantial upsurge in AWD. In contrast, the Hotan region witnessed a reduction in high
538 evapotranspiration cotton cultivation, along with an increase in wheat and maize cultivation,
539 thereby maintaining overall AWD at a controlled leve across the entire region.

540 The increase in domestic and production water will inevitably displace ecological water.
541 The natural oases exhibited varying degrees of retreat. EWD in the Aksu and Hotan regions
542 decreased significantly by 2010, aligning with the shrinking trend of natural oases. In Kashgar,
543 despite the continuous reduction in the area of natural oases EWD
544 increased[$(0.12\pm0.09)\times10^8 m^3/a(P<0.1)$]. This was due to a substantial decline in the area of
545 shrub forests, sparse woodlands, and low-coverage grasslands with low evapotranspiration, while
546 the area of high-coverage grassland with high evapotranspiration has increased.

547 3.4 Present situation analysis and prediction of water stress in TRSX

548 By using the water supply and water demand data of the study area, we can analyze the
549 relationship between water resource supply and demand and water stress in the historical period
550 of TRSX.

Regarding water supply, the available water in TRSX showed a significant increasing trend. The water availability in Aksu, Kashgar, and Hotian regions is (138.22±23.55) $\times10^8m^3/a$, (90.67±17.12) $\times10^8m^3/a$, and (23.91±7.56) $\times10^8m^3/a$, respectively. The average annual increase was (0.69±0.16) $\times10^8$m3/a (P<0.01), (0.36±0.12) $\times10^8m^3/a$ (P<0.01) and (0.21±0.05) $\times10^8m^3/a$ (P<0.01), respectively. Concerning water demand, there are significant regional differences in the total water demand of the TRSX. The total water demand in Aksu and Kashgar regions is (131.20±15.13) $\times10^8m^3/a$ and (130.56±17.67) $\times10^8$m3/a$\times10^8m^3/a$, respectively. The total water demand in the Hotian region is relatively lower (27.13±1.68) $\times10^8m^3/a$, and the water demand in the Aksu and Kashgar regions is on the rise. The average annual increase was (2.34±0.20) $\times10^8m^3/a$ (P<0.01) and (2.56±0.32) $\times10^8m^3/a$ (P<0.01), respectively, while the average annual decrease was (-0.14±0.06) $\times10^8m^3/a$ (P<0.05).

Based on the available water and total water demand in TRSX, we can obtain the multi-year average water stress status and change trend of TRSX from 2000 to 2020 by using the WSI method and classifying water stress according to Falkenmark. Aksu, Kashgar and Hotan regions all experienced high levels of water stress and extremely high levels of water stress, with water stress indices of 0.40±0.17, 0.63±0.18, and 0.89±0.30, respectively. Although TRSX as a whole showed a high level of water stress, different regions exhibited different changing trends. As shown in Figure 6, the water stress increased in Aksu and Kashgar regions but decreased in the Hotan region.

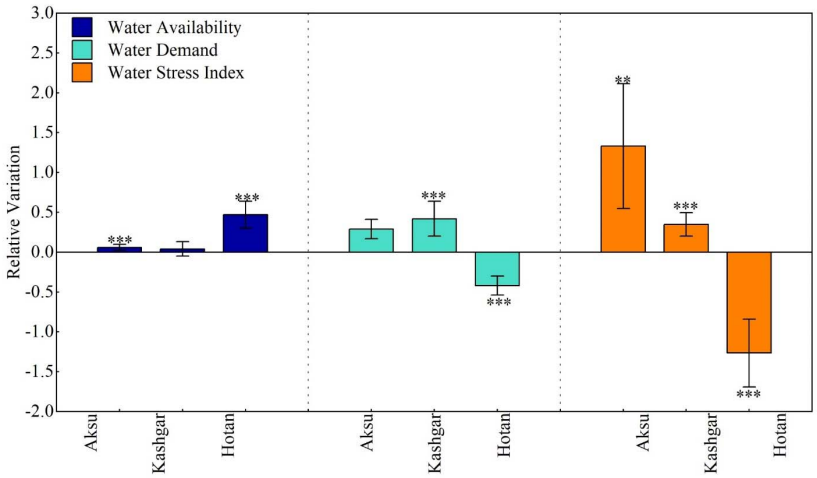

Note: * is represented as P<0.1, ** as P<0.05, *** as P<0.01, sd as standard deviation.

Fig6. Relative variation ratio of water availability, water demand and water stress index in southern Xinjiang from 2000 to 2020

The prediction of future water stress in TRSX is based on the analysis of future water availability and water demand data in the regions. Future water availability in the region is calculated as the predicted total runoff minus the runoff required to maintain the discharge of the mainstream of the Tarim River, taking into account the utilization rate of water resources in each region. The total runoff includes future glacier meltwater simulated by a degree-day model, predicted precipitation based on current trends, and a fixed proportion of groundwater. Future water demand in the region includes domestic, industrial, livestock, agricultural, and ecological uses. Domestic water demand is predicted based on the population increase trend in Xinjiang

outlined in the *White Paper on Population Development of Xinjiang*. Industrial and livestock water demand is estimated according to the industrial output value targets and livestock breeding plans set in *the 14th Five-Year Plan for National Economic and Social Development and the Outline of Long-term Goals for 2035 in the region*. Agricultural water demand is projected, assuming the existing cultivation area and planting structure remain unchanged. Ecological water demand is estimated based on the existing natural oasis area. Using the years 2000-2020 as a reference, we calculate the annual average water availability and water demand of TRSX under the SSP2-4.5 and SSP5-8.5 scenarios in CMIP6. Additionally, we calculate the change in the average water stress of each region under the corresponding scenarios and periods.

The results indicate that (Figure7.), compared to the average value of the reference period (2000-2020), water availability in TRSX will not continue to increase in the next two scenarios, while the water demand will essentially increase. Under the SSP2-4.5 scenario, water availability in the Aksu and Kashgar regions continues to increase from 2030s to 2070s but shows a downward trend in the 2090s. The Hotan region shows little change in the 2030s compared to the reference period (with an increment of less than 5%), and then exhibits a continuous upward trend. Under the SSP5-8.5 scenario, water availability in the Aksu region increases from the 2030s to the 2090s and then declines. From the 2030s to the 2090s, the water volume in Kashgar increased. The Hotan region does not change significantly in the 2030s and continues to rise thereafter. In terms of water demand, under both scenarios, except for the Hotan region, which remains unchanged from the reference period in the 2030s, other regions show a continuous upward trend in each period.

The change in water availability and water demand leads to a change in the water stress index. As shown in Figure 5, in the Aksu region, the water stress index is greater than the reference period level in both scenarios, but the increase decreases with time. In the Kashgar region, under the SSP2-4.5 scenario, the water stress index is greater than the reference period level, but the increase continues to decrease before the 2070s, and then rises again in the 2090s. Under the SSP5-8,5 scenario, the water stress index continues to decrease and is less than the reference period level after the 2070s. In the Hotan region, the water stress index continues to decrease in the next two scenarios and is less than the reference period level. Compared with the SSP2-4.5 scenario, the SSP5-8.5 scenario exhibits a larger decrease. In general, the changes in the water stress index in TRSX are not consistent. In the Aksu region, although future water availability and total water demand are continuously increasing, the increase in total water demand is much greater than that in water availability, resulting in a rising water stress index. In the Kashgar region, the increase in water availability is less than that in water demand under the SSP2-4.5 scenario, leading to an increased water stress index. In the 2070s and 2090s, the increase in water availability wa greater than that in water demand under the SSP5-8.5 scenario, resulting in a decreased water stress index. In the Hotan region, the increase in water availability exceeds that in water demand, leading to decreased water stress index.

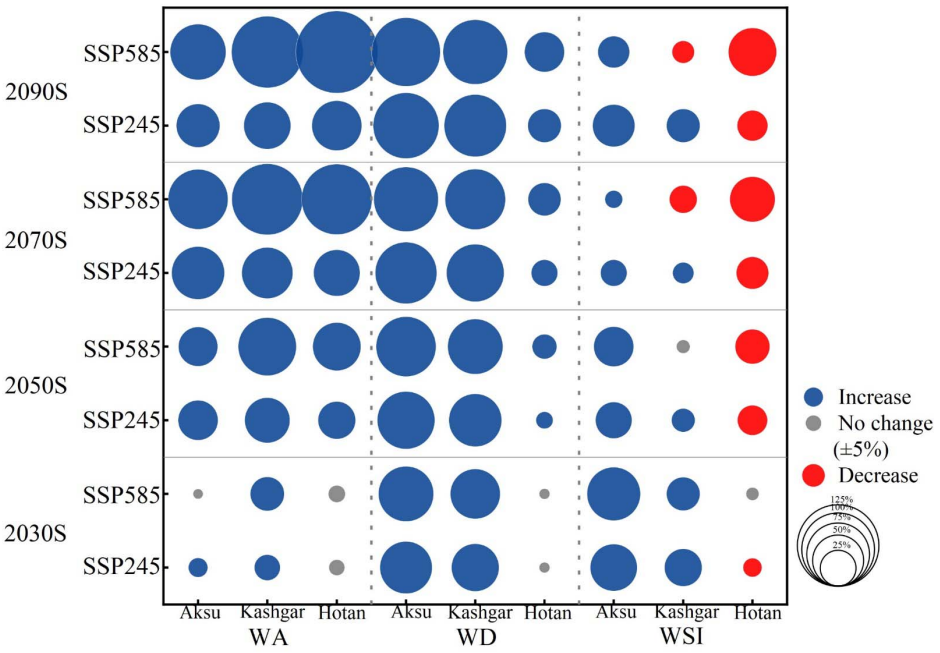

Fig7. Changes of water availability, water demand and water stress index in TRSX in different periods under future scenarios

4.Discussion

The water stress calculated through the water stress index (WSI) hinges on both water availability and total water demand. Thus, the factors influencing water availability and total water demand in TRSX are critical in determining water stress. This study utilizes meteorological data, land use data, socio-economic data, and natural phenology data to calculate average water availability, total water demand, and water stress in TRSX over several years. It also investigates the primary drivers behind water stress in region.

The surface runoff in TRSX is primarily supplied by precipitation and glacier meltwater. In recent years, due to the influence of global climate change, there has been a significant shift in water resource availability in TRSX, resulting in a notable increase in the overall water supply This transformation is attributed in part to increased precipitation, but the major contributor is the melting of glaciers in the surrounding mountainous areas. As glacier meltwater continues to accumulate in the basin, both runoff and water availability rise. Consequently, the increase in water availability under the SSP5-8.5 scenario exceeds that in the SSP2-4.5 scenario. However, as temperatures continue to rise and glaciers continue to shrink, the glacier area will gradually decrease, leading to a peak in glacier meltwater volume, followed by a decline (Figure 8). This reduction in glacier meltwater will result in decreased water availability and, consequently, increased water stress in the region. Additionally, glacial meltwater assumes a more significant role during dry years. In an average year, the precipitation in the Aksu, Weigan, Yarkand, Hotan and Kriya Rivers accounts for 20.63%, 15.41%, 16.56%, 16.31%, and 16.05% of the total runoff, respectively, while glacial meltwater contributes 55.67%, 31.19%, 60.84%, 58.69%, and 64.95%, respectively. However, during typical dry years, precipitation reduces significantly. In these dry years, temperatures are higher compared to an average year, resulting in even greater

glacier melting and an increase in glacier meltwater. The percentages of glacial meltwater increased significantly, reaching 68.38%, 38.81%, 72.05%, 72.07%, and 78.92%, respectively, representing an increase of 7.62% to 13.97% over the average year (Figure 9).

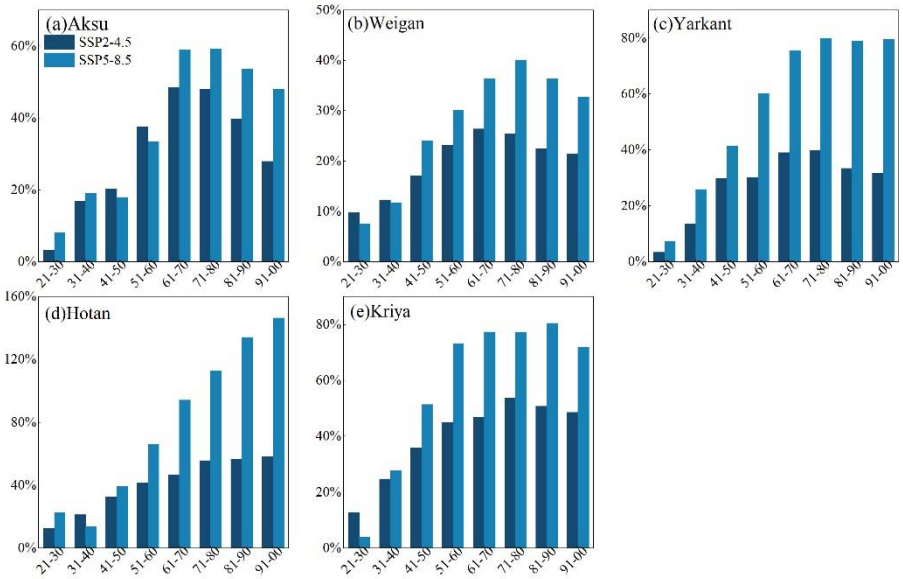

Fig8. The increase of glacial meltwater in the two scenarios compared with the reference period (2000-2019)

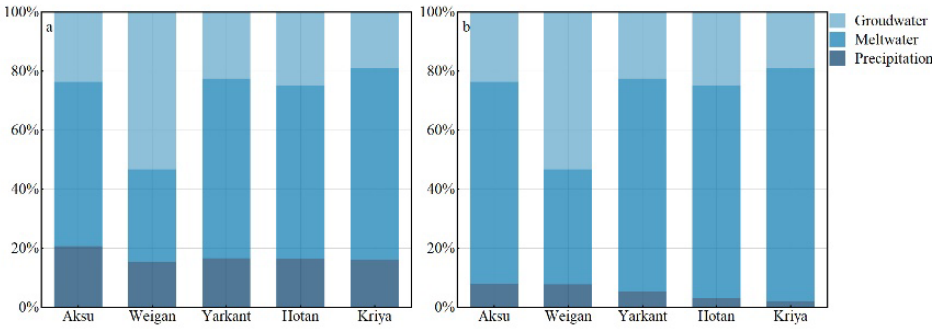

Fig9. Ratio of runoff composition in average years and drought years

The total water demand in this study includes five components: domestic water demand, industrial water demand, livestock water demand, agricultural water demand and ecological water demand. DWD depends on both population and domestic water intensity (per capita water consumption per unit of time). IWD is calculated based on industrial output value, industrial water intensity (water consumption per unit of output value), and water efficiency coefficient. LWD is analogous to DWD, relying on the livestock numbers and livestock water intensity (livestock water usage per unit of time). AWD hinges on the crop type, area, crop evapotranspiration, and irrigation efficiency coefficient. EWD is contingent on vegetation type, area, vegetation coefficient, and actual evapotranspiration. Agricultural water constitutes the predominant part of total water demand, with the amount of agricultural water being directly proportional to cultivated land area. Consequently, an increase in the cultivated land area of the region leads to a corresponding increase in the region's total water demand, thus making

agriculture the determinant of the region's overall water demand. Additionally, factors such as the TRSX population, industrial and animal husbandry development, and natural oasis area changes exert a certain, albeit minor, influence on the region's total water demand. The occurrence of water stress in TRSX is influenced by alterations in water availability due to climate change, and human activities related to total water demand, based on the interplay between the region's hydrothermal conditions and human water intake.

This study evaluated the historical water stress status and changes in TRSX concerning water availability and total water demand. It also predicted water stress changes for the next four periods under the two scenarios of SSP2-4.5 and SSP5-8.5 in the CMIP6 model, shedding light on the trends of water stress alterations in TRSX, both presently and in the future. This analysis is beneficial for guiding the formulation of regional water resources management policies. High water stress in TRSX arises from a combination of limited water availability, and increases total water demand due to socioeconomic development. Hence, regional water resource management policies should address both the water supply and demand sides of the equation.

In the future, TRSX will continue to experience warming climates, ongoing glacier melting, and an increasing volume of glacial meltwater. Simultaneously, water demand will sharply rise, posing substantial challenges to water resources management. In the short term, the trend of climate warming cannot be reversed, but sustainable water resource utilization can be achieved by restricting human activities. The primary factor driving increased water consumption in TRSX is the expansion of cultivated land associated with increased AWD. Therefore, controlling cultivated land area should be a top priority. The scale of suitable arable land has been estimated in some areas, suggesting that the Aksu Oasis should reduce its farmland by26% based on its existing scale (Wang et al., 2019), while 1487 km^2 of farmland should be abandoned in the Yarkant River Basin, and 238 km^2 in the Hotan River Basin (Chen et al., 2013). The area of cultivated land in the Kriya River Basin should be regulated between 158.69 and 263.65 km^2 (Zubaidai, 2019). Secondly, irrigation water efficiency should be improved through the use of plastic-film-covered and drip irrigation technology. Studies have shown that increasing irrigation water efficiency from 0.42 to 0.55 in Northwest China can reduce AWD by 12.3-13.0$\times10^8$ m^3 (Guo and Shen, 2016). Thirdly, the exploitation of groundwater should be controlled, surplus surface water during wet years should be recharged to groundwater, and the concept of "underground reservoir" should replace glacier "solid reservoir" to prevent water resource security crises during extreme drought conditions.

During drought years, especially during multi-year droughts, the limited precipitation cannot meet the oasis's water demand. If glaciers disappear in the future, and in the case of extremely low precipitation (referring to precipitation data from the least precipitation years in the past 60 years), it is essential to prioritize DWD, LWD, and EWD. DWD and LWD are essential for human survival, while EWD is crucial for maintaining the ecological interity of the oasis. Any surplus water should be allocated to industry use. Therefore, the minimum water requirements in the Aksu, Kashgar and Hotan regions are 13.28$\times10^8$ m^3, 15.36$\times10^8$ m^3, and 9.84$\times10^8$ m^3, respectively. Furthermore, considering the annual precipitation over the past 60 years, TRSX experiences five-year dry periods. Consequently, it is recommended that the water in the three regions reserve the most basic amount of water (i.e., DWD, LWD, EWD) for at least four to five years, with respective volumes of 36.84$\times10^8$ m^3, 52.64$\times10^8$ m^3, and 46.15$\times10^8$ m^3, to ensure sustainable oasis development of the oasis even during consecutive dry years.

Although the calculation of water availability and total water demand incorporates various data, this study still has some uncertainties in its results. These primarily include: (1) In the simulation of glacier meltwater, precipitation in the glacier area is obtained through interpolation from meteorological stations to the glacier's end, and the precipitation gradient is used to estimate precipitation from the glacier's end to the glacier area. Both methods may not accurately represent spatial variations in precipitation in the glacier area. (2) The predicted runoff calculates groundwater in a fixed proportion, which could result in overestimating the results. (3) The forecast of future total water demand in this study does not consider changes in agricultural planting area and natural vegetation area, potentially introducing bias into results. (4) The study only focuses on the quantity of water resources in the study area and does not account for water quality, which may result in a lower calculated water pressure value. In reality, the region may experience higher water pressure due to the water quality issues.

5 Conclusions

In conclusion, this paper, focusing on the perspective of supply and demand, assesses historical and future water stress in the Aksu, Kashgar, and Hotan s of TRSX using the classical water stress index method. It thoroughly analyzes the changes in both supply and demand that contribute to water stress and identifies regional variations. The findings provide a scientific foundation for managing, planning, and policymaking regarding water resources in these regions, contributing to the sustainable development of water resources and the local economy. The key conclusions are as follows:

(1) From 1961 to 2020, TRSX experienced significant changes in water resources. Precipitation in the region increased, and the glacier meltwater showed an upward trend due to rising temperatures. These dual effects resulted in a notable increase in river runoff, leading to greater water availability.

(2) Between 2000 and 2020, the Aksu and Kashgar regions witnessed a substantial rise in total water demand, primarily driven by increased agricultural water needs. In contrast, the Hotan region saw a decrease in total water demand due to maintaining the original level of agricultural water demand and a significant drop in ecological water demand.

(3) Throughout the period from 2000 to 2020, all of TRSX experienced high levels of water stress. Despite the overall increase in water availability, the level of water stress varied significantly due to inconsistent changes in total water demand. Aksu and Kashgar regions witnessed an escalating water stress level attributed to the substantial increase in water demand, while the Hotan region experienced some relief owing to reduced water demand but still faced with a high level of water stress.

(4) Compared to the historical period (2000-2020), projections for the next four periods (2030s, 2050s, 2070s, and 2090s) under the SSP2-4.5 and SSP5-8.5 scenarios in the CMIP6 model reveal an increase in both water availability and water demand in TRSX. However, the rate of increase varies. In the Aksu region, both water availability and water demand will continue to rise in the future, with the increase in water demand surpassing that of water availability, leading to a continuous rise in the WSI. In the Kashgar region, under the SSP2-4.5 scenario, the increase in water availability is less than that of water demand, resulting in an increased WSI. However, in the 2070s and 2090s, under the SSP5-8.5 scenario, the increase in

749 water availability exceeds that of water demand, leading to a decreased WSI. In Hotan, the
750 increase in water availability surpasses that of water demand, resulting in a decrease in the WSI.

751 **Acknowledgments**

752 We thank Dr. Dong Chen and Dr. Chiyuan Miao for guidance on the research, Dr.
753 Chiyuan Miao for providing the processed CMIP6 climate data.

754 **Data Availability Statement**

755 The socio-economic data is available at the Xinjiang Statistical Yearbook and the "*Notice*
756 *on Printing and Distributing Industrial and Domestic Water Quotas in Xinjiang Uygur*
757 *Autonomous Region*". The meteorological data is available at the National Meteorological
758 Science Data Center (http://data.cma.cn/) and the Resource and Environment Science and Data
759 Center (http://www.resdc.cn/). The phenological data is collected from Food and Agriculture
760 Organization of the United Nations (FAO). The oasis land use data is provided by the Geospatial
761 Data Cloud (https://www.gscloud.cn), the 30 m global surface coverage is provided by the
762 National Catalogue Service for Geographic Information (https://www.webmap.cn).
763

764 **References**

765 Bach, E., Radic, V., Schoof, C. 2018, How sensitive are mountain glaciers to climate change?
766 Insights from a block model. Journal of glaciology, 64(244):247-258.
767 https://doi.org/10.1017/jog.2018.15
768 Chen, R., Song, Y., Kang, E., Han, C., et al., 2014. A Cryosphere-Hydrology Observation
769 System in a Small Alpine Watershed in the Qilian Mountains of China and Its Meteorological
770 Gradient. Arctic, antarctic, and alpine research, 46(2): 505-523. https://doi.org/10.1657/1938-
771 4246-46.2.505
772 Chen, W., Lu, Y., Liu, G., 2022, Balancing cropland gain and desert vegetation loss: The key to
773 rural revitalization in Xinjiang, China. Growth and Change, 53(3):1122-1145.
774 https://doi.org/10.1111/grow.12568
775 Chen, Y., Ye, Z., Shen, Y., 2011. Desiccation of the Tarim River, Xinjiang, China, and
776 mitigation strategy. Quaternary International, Vol. 244 No. 2, pp. 264-271.
777 https://doi.org/10.1016/j.quaint.2011.01.039
778 Cheng, H., Hu, Y., Zhao, J., 2009. Meeting China's water shortage crisis: current practices and
779 challenges. Environmental science & technology, 43(2):240-244.
780 https://doi.org/10.1021/es801934a
781 Gosling S N, Arnell N W. Global assessment of the impact of climate change on water
782 scarcity[J]. Climatic change, 2016,134(3):371-385. https://doi.org/10.1007/s10584-013-0853-x
783 Liu X, Liu W, Yang H, et al. Multimodel assessments of human and climate impacts on mean
784 annual streamflow in China[J]. Hydrology and earth system sciences, 2019,23(3):1245-1261.
785 https://doi.org/10.5194/hess-2018-525
786 Duan, Z., Ni, M., Tao, Y., Marcin, S., Xia, J. 2021. Impact of climate change and human
787 activities on the sustainable development of Xinjiang Aksu Oasis (China). Acta Sci Pol.
788 Formatio Circumiectus, 20(2):3-18. https://doi.org/10.15576/ASP.FC/2021.20.2.3

789 Guo, Y., Shen, Y. 2016, Agricultural water supply/demand changes under projected future
790 climate change in the arid region of northwestern China, Journal of Hydrology, 540:257-273.
791 https://doi.org/10.1016/j.jhydrol.2016.06.033
792 Deng, H., Chen, Y., Li, Y. 2019. Glacier and snow variations and their impacts on regional water
793 resources in mountains. Journal of Geographical Sciences, 29(1), 84-100.
794 https://doi.org/10.1007/s11442-019-1585-2
795 Tao, H., Gemmer, M., Bai, Y., et al., 2011. Trends of streamflow in the Tarim River Basin
796 during the past 50 years: human impact or climate change? Journal of Hydrology, 400(1-2):1-9.
797 https://doi.org/10.1016/j.jhydrol.2011.01.016
798 Huss, M., & Hock, R. 2018. Global-scale hydrological response to future glacier mass loss.
799 Nature Climate Change, 8(2):135–140. https://doi.org/10.1038/s41558-017-0049-x
800 Immerzeel, W. W., van Beek, L. P. H., Bierkens, M. F. P. 2010.Climate Change Will Affect the
801 Asian Water Towers. Science, 328(5984):1382–1385. https://doi.org/10.1126/science.1183188.
802 IPCC 2019, Special Report: The Ocean and Cryosphere in a Changing Climate—Summary for
803 Policymakers. WMO/UNEP.
804 Ling, H., Xu, H., & Fu, J. 2012. High- and low-flow variations in annual runoff and their
805 response to climate change in the headstreams of the Tarim River, Xinjiang, China. Hydrological
806 Processes, 27(7):975–988. https://doi.org/10.1002/hyp.9274.
807 Liu, Y., Xue, J., Gui, D., et al., 2018. Agricultural Oasis Expansion and Its Impact on Oasis
808 Landscape Patterns in the Southern Margin of Tarim Basin, Northwest China. Sustainability,
809 10(6):1957. https://doi.org/10.3390/su10061957.
810 Penna, D., Engel, M., Mao, L., et al., 2014. Tracer-based analysis of spatial and temporal
811 variations of water sources in a glacierized catchment. Hydrology and Earth System Sciences,
812 18(12):5271–5288. https://doi.org/10.5194/hess-18-5271-2014.
813 Piao, S., Ciais, P., Huang, Y., et al., 2010. The impacts of climate change on water resources and
814 agriculture in China. Nature, 467(7311):43–51. https://doi.org/10.1038/nature09364.
815 Pritchard, H. D. 2019. Asia's shrinking glaciers protect large populations from drought stress.
816 Nature, 569(7758):649–654. https://doi.org/10.1038/s41586-019-1240-1.
817 Rounce, D. R., Hock, R., Shean, D. E. 2020. Glacier mass change in high mountain asia through
818 2100 using the open-source python glacier evolution model (pygem). Frontiers in Earth Science,
819 7, 331. https://doi.org/10.3389/feart.2019.00331.
820 Zhang, S., Gao, X., Zhang, X., et al., 2012. Projection of glacier runoff in Yarkant River basin
821 and Beida River basin, Western China. Hydrological Processes, 26(18):2773–2781.
822 https://doi.org/10.1002/hyp.8373.
823 Sorg, A., Bolch, T., Stoffel, M., et al., 2012. Climate change impacts on glaciers and runoff in
824 Tien Shan (Central Asia). Nature Climate Change, 2(10):725–731.
825 https://doi.org/10.1038/nclimate1592.
826 Sun, J., Wang, X., Cao, Y., et al., 2018. Analysis of spatial and temporal evolution of
827 hydrological and meteorological elements in Nenjiang River basin, China. Theoretical and
828 Applied Climatology.137. https://doi.org/10.1007/s00704-018-2641-z.
829 Tang, Q., Liu, X., Zhou, Y., et al., 2022). Climate change and water security in the northern
830 slope of the Tianshan Mountains", Geography and Sustainability, 3(3):246-257.
831 https://doi.org/10.1016/j.geosus.2022.08.004
832 Torrence, C., Compo, G. P., 1998. A Practical Guide to Wavelet Analysis. Bulletin of the
833 American Meteorological Society, 79(1):61–78. https://doi.org/10.1175/1520-
834 0477(1998)079<0061: apgtwa>2.0.co;2.

Wang, Y., Li, C., Ochege, F., et al., 2022. Contribution of cropland expansion to regional carbon stocks in an arid area of China: a case study in Xinjiang, Carbon Management, 13(1):42-54. https://doi.org/10.1080/17583004.2022.2043446

Yang, P., Zhang, S., Xia, J., et al., 2022. Risk assessment of water resource shortages in the Aksu river basin of northwest China under climate change. Journal of Environmental Management, 305, 114394. https://doi.org/10.1016/j.jenvman.2021.114394

Zhang, Q., Chen, Y., Li, Z., et al., 2019. Glacier changes from 1975 to 2016 in the Aksu River Basin, Central Tianshan Mountains. Journal of Geographical Sciences, 29(6):984–1000. https://doi.org/10.1007/s11442-019-1640-z.

Zhang, Y., Liu, S., Xu, J., et al., 2007. Glacier change and glacier runoff variation in the Tuotuo River basin, the source region of Yangtze River in western China. Environmental Geology, 56(1):59–68. https://doi.org/10.1007/s00254-007-1139-2.

Zhao, Q., Zhang, S., Ding, Y., et al., 2015. Modeling Hydrologic Response to Climate Change and Shrinking Glaciers in the Highly Glacierized Kunma Like River Catchment, Central Tian Shan. Journal of Hydrometeorology, 16(6):2383–2402. https://doi.org/10.1175/jhm-d-14-0231.1.

Zhou, D., Wang, X., Shi, M. 2016. Human Driving Forces of Oasis Expansion in Northwestern China During the Last Decade-A Case Study of the Heihe River Basin. Land Degradation & Development, 28(2):412–420. https://doi.org/10.1002/ldr.2563.

Zubaidi, M., Xia, J., Polat, M., et al., 2018. Spatiotemporal changes of land use/cover from 1995 to 2015 in an oasis in the middle reaches of the Keriya River, southern Tarim Basin, Northwest China", Catena, 171:416-425. https://doi.org/10.1016/j.catena.2018.07.038.

Cao, Z., Wang, X., Li, W., et al., 2012. Suitable scale for oasis in lower reaches of Tarim River, Arid Land Geography, 35(05):806-814. https://doi.org/10.13826/j.cnki.cn65-1103/x.2012.05.013

Chen, Y., Chen, Z., 2013, Analysis of oasis evolution and suitable development scale for arid regions: a case study of the Tarim River Basin, Chinese Journal of Eco-Agriculture, 21(01), pp. 134-140. https://doi.org/10.3724/SP.J.1011.2013.00134

Ding, Y., Zhao, Q., Wu, J., et al., 2020, The future changes of Chinese cryospheric hydrology and their impacts on water security in arid areas. Journal of Glaciology and Geocryology, 42(01): 23-32. https://doi.org/10. 7522/j. issn. 1000-0240. 2020. 0003

Gao, X., Ye, B., Zhang, S., et al., 2010. Glacier runoff variation and its influence on river runoff during 1961–2006 in the Tarim River Basin. China. Sci: China Earth Sci, 53:880-891 https://doi.org/10.1007/s11430-010-0073-4.

Gao, X., Zhang, S., Ye, B., et al., 2010. Glacier Runoff Change in the Upper Stream of Yarkant River and Its Impact on River Runoff during 1960-2006, Journal of Glaciology and Geocryology, 32 (03):445-453. https://doi.org/10.1017/S0004972710001772

Han, R., Zhao, Z., Xiao, N., et al., 2020. Analysis on the Land Use Change and Its Driving Forces in Southern Region of Xinjiang Province during 2010-2015, Bulletin of Science and Technology, 36(02):24-31. https://doi.org/10.13774/j.cnki.kjtb.2020.02.004

He, K., Wu, S., Yang, Y., et al., 2018. Dynamic changes of land use and oasis in Xinjiang in the last 40 yeares, Arid Land Geography, 41(6):1333-1340. https://doi.org/10.12118/j.issn.1000-6060.2018.06.21.

Huang, Y., Xiao, C., Su, B., et al. 2020. Importance of cryosphere water resources to China's socio-economy: Based on multi-level basins analysis (in Chinese). Chin Sci Bull, 65: 2636–2650, https://doi.org/10.1360/TB-2020-0073.

Kang E., 2002. Ice and snow water resources and mountain runoff in arid area of northwest China. Beijing: Science Press:14-54

Liu, S., Yao, X., Guo, W., et al., 2015. The contemporary glaciers in China based on the Second Chinese Glacier Inventory. Acta Geographica Sinica, 70(01):3-16 https://doi.org/10.11821/dlxb201501001

Lv, N., Bai, J., Chang, C., et al., 2017 Spatial-temporal changes in evapotranspiration based on planting patterns of major crops in the Xinjiang oasis during 1960-2010. Geographical Research, 36(08):1443-1454. https://doi.org/10.11821/dlyj201708004

Ren, X., Mu, G., Xu, L., et al., 2015 Characteristics of artificial oasis expansion in south Traim Basin from 2000-2013. Arid Land Geography, 38(5):1022-1030. https://doi.org/10.13826/j.cnki.cn65-1103/x.2015.05.017

Shangguan, D., 2007 Application research to glacier change in Tarim River Basin based on 3S. Cold and Arid Regions Environmental and Engineering Research Institute, Chinese Academy of Sciences.

Shen Y., Su H., Wang G., et al. The responses of glaciers and snow cover to climate change in Xinjiang(I): hydrological effect. Journal of Glaciology and Geocryology. 2013, 35(03):513-527 https://doi.org/10.7522/j.issn.1000-0204.2013.0061

Shen, Y., Wang, S., 2002, New progress in Glacier and Water Resources Changes in Tarim Basin, Xinjiang. Journal of Glaciology and Geocryology, 24(06):819.

Wang, Z., Jiang, J., Fang, G., 2019, Analysis on the suitable scale of the Aksu Oasis under the limit of water resources. Journal of Glaciology and Geocryology, 41(04):986-992. https://doi.org/10. 7522/j. issn. 1000-0240. 2019. 0046

Xie, Z., Wang, X., Kang, E., et al., 2006. Glacial Runoff in China: An Evaluation and Prediction for the Future 50 Years. Journal of Glaciology and Geocryology. 28(4): 457—466 https://doi.org/10.3969/j.issn.1000-0240.2006.04.001

Xu, A., 2017, Monitoring glacier change based on remote sensing in China Karakoram for the last four decades. Lanzhou University. https://doi.org/10.7666/d. D01300462

Zhang, S., 2008.Research of Surface Water Resources in Xinjiang Uygur Autonomous Region, China Water & Power Press

Zhuang, Q., Wu, S., Luo, G., et al., 2020 Changes in oasis and coordination of resource allocation in Xinjiang, Arid Land Geography, 43(5):1298-1306. https://doi.org/10.12118/j.issn.1000－6060.2020.05.15

Zubaidai, M., 2019 Study on Land use/cover Change and its Sustainability in Kriya River Basin, Xinjiang. Minzu University of China. https://doi.org/10.27667/d.cnki.gzymu.2019.000002

Zuo, J., Assessment of the uncertainty of runoff and the water shortage risk in the Tarim River basin under the impact of climate change. East China Normal University, 2021 https://doi.org/10.27149/d.cnki.ghdsu.2021.000391

Alcamo J， Thomas T， Rösch T. World water in 2025： global modeling and scenario analysis for the World Commission on Water for the 21st century［J］. Kassel World Water，1999， 15 （28）： 32-41. https://doi.org/10.1108/IJCST-10-2014-0123

Munia H, Guillaume J H A, Mirumachi N, et al. Water stress in global transboundary river basins: significance of upstream water use on downstream stress[J]. Environmental Research Letters, 2016, 11(1):014002. https://doi.org/10.1088/1748-9326/11/1/014002